Contract No:

This document was prepared in conjunction with work accomplished under Contract No. 89303321CEM000080 with the U.S. Department of Energy (DOE) Office of Environmental Management (EM).

Disclaimer:

A U.S. DEPARTMENT OF ENERGY NATIONAL LAB • SAVANNAH RIVER SITE • AIKEN, SC • USA

Destructive Examination of Shipping Package 9975-02731

T. T. Truong

Z. Lowe

June 2022

SRNL-STI-2022-00234, Revision 0

DISCLAIMER

Printed in the United States of America

Prepared for
U.S. Department of Energy

SRNL-STI-2022-00234
Revision 0

Keywords: *K-Area Surveillance*
9975 Shipping Package

Retention: *Permanent*

Destructive Examination of Shipping Package 9975-02731

T. T. Truong
Z. Lowe

June 2022

Savannah River National Laboratory is operated by Battelle Savannah River Alliance for the U.S. Department of Energy under Contract No. 89303321CEM000080.

REVIEWS AND APPROVALS

AUTHORS:

T. T. Truong, Separation Sciences & Engineering Date

Z. Lowe, Separation Sciences & Engineering Date

TECHNICAL REVIEW:

M. D. Kranjc, Materials Evaluation & NDE Date

APPROVAL:

R. E. Fuentes, Pu Surveillance Program Lead, Separation Sciences & Engineering Date

B. J. Wiedenman, Manager Date
Chemical Processing and Characterization

A. J. O'Grady, KAC Process Support Engineering Date

D. R. Leduc, Packaging Technology Date

EXECUTIVE SUMMARY

Destructive and non-destructive examinations were performed on the components of the package 9975-02731 as part of a comprehensive Savannah River Site surveillance program for plutonium materials stored in the K-Area Complex (KAC). The package stored nuclear materials in KAC for 13.8 years. Inspection of the package during opening in KAC noted one non-conforming condition: a large discolored area on the upper fiberboard subassembly. The package was subsequently transferred to Savannah River National Laboratory for more detailed examination. In addition to the observation noted in KAC, the following conditions were observed:

- Axial gap of 1.021 inch slightly exceeded the 1 inch maximum criterion
- Lead shield height exceeded drawing tolerance of 24.7 inch by 0.019 inch.

Visual examination of the upper fiberboard assembly and analysis of the discolored fiberboard indicate the discoloration was due to wood glue residue. The physical, thermal, and mechanical properties of the fiberboard met the acceptance criteria and/or were within the range of previously tested fiberboard and baseline samples. The visual, microscopic and tensile testing results were consistent with previous O-ring and baseline Viton results. The lead shield surface was covered with corrosion product as observed on other shields but there was no evidence of excessive blistering, flaking, or spalling. Besides minor and expected corrosion, no evidence of a degraded condition was found in this package. Examination of the 9975-02731 corroborates existing evidence that the 9975 package is robust and the components can perform their expected functions.

TABLE OF CONTENTS

LIST OF TABLES

LIST OF FIGURES

LIST OF ABBREVIATIONS

ASTM	American Society for Testing Materials
DE	Destructive Examination
DSA	Documented Safety Analysis
EDS	Energy-dispersive X-ray Spectroscopy
FTIR	Fourier Transform Infrared
ID	Inside Diameter
KAC	K-Area Complex
MTE	Measuring and Test Equipment
OD	Outside Diameter
PCV	Primary Containment Vessel
RH	Relative Humidity
SCV	Secondary Containment Vessel
SEM	Scanning Electron Microscopy
SRNL	Savannah River National Laboratory
SRS	Savannah River Site
WME	Wood Moisture Equivalent

1.0 Introduction

Savannah River Site (SRS) stores plutonium materials within model 9975 shipping packages in the K-Area Complex (KAC). The 9975 shipping package consists of a 35 gallon stainless steel drum, Celotex® fiberboard insulation, lead shield, and primary and secondary containment vessels. The 9975 shipping package design, performance, and analysis for safe transport of radioactive materials are described in the Safety Analysis Report for Packaging (SARP) [1]. The KAC Documented Safety Analysis (DSA) credits the 9975 shipping package to perform several safety functions, including containment, criticality prevention, and fire resistance to prevent release of special nuclear materials [2].

The 9975 shipping packages with 3013 containers are expected to perform its safety functions for at least 20 years in the KAC storage environment [3-4], and was recently assessed for a 40-year storage life in KAC [5]. The storage of 9975 shipping packages with non-3013 containers have been evaluated for 20 years of storage [6]. The DSA recognizes the potential for material degradation over time and requires an assessment of materials performance to validate the assumptions for extended storage in KAC. The SRS Surveillance Program monitors material performance to establish a basis for service life and ensures the continued integrity of 9975 packages. As part of the Surveillance Program [7-8], destructive examination (DE) of package 9975-02731 was performed in accordance with the task plan [9].

2.0 Experimental Procedure

2.1 Package History and Opening

Package 9975-02731 was loaded with special nuclear materials at Hanford Site and received in KAC in November 2007. The contents generated 3.0 watts heat load. Routine package opening was performed on August 18, 2021 after 13.8 years. During unpackaging, a large discoloration, approximately 8" wide, was observed on the upper fiberboard assembly. The unknown substance was not wet or contaminated. The discoloration was not observed on the lower fiberboard assembly. Subsequently, the package was transferred to Savannah River National Laboratory (SRNL) for additional analysis and destructive examination.

As the package was first opened in SRNL and components removed, each component was marked to identify its orientation within the package. For components that were removed during unpackaging, their orientation at SRNL examination probably bears no relation to their orientation while stored in KAC. However, the bottom fiberboard subassembly and lead shield would likely have remained in the same orientation they occupied in KAC.

Examination activities are documented through photographs, data sheets, and observations in an electronic laboratory notebook [10].

2.2 Package Examination

Visual examination: All package components were examined for damage or degradation, with a primary focus on fiberboard subassemblies, O-rings, and lead shield. Pictures were taken of the package materials and any atypical conditions (*e.g.,* dents or corrosion on the drum).

Fiberboard physical properties & moisture content: The weight and dimensions of the two fiberboard subassemblies were measured in SRNL 76 days after unpackaging in KAC. The fiberboard subassemblies' volume and density were calculated using nominal values for the air shield and aluminum bearing plates. Moisture content, in wood moisture equivalent (WME), was measured using a GE Protimeter Surveymaster moisture meter. WME is the weight percent of moisture that would produce the same electrical conductivity in wood. The relative humidity (RH) of the air was measured using a Rotronic Hygropalm HP21 meter.

The correlation between moisture content of fiberboard and humidity in the drum was examined. A narrow channel was cut down the side of the lower subassembly to fit the Hygropalm meter. The drum was closed, and the humidity readings were taken at several locations along the subassembly after the humidity levels inside the drum reached equilibrium (*e.g.,* after 2 days). The lower subassembly was removed from the drum and the moisture content was measured at those same locations. Humidity values were converted to equivalent relative humidity at 21 °C to compare data from various packages as relative humidity is temperature dependent.

Fiberboard thermal and mechanical properties: Samples were removed from the side and base of the lower subassembly to measure compressive strength, specific heat capacity, and thermal conductivity of fiberboard as illustrated in Figure 1. The thermal conductivity sample from the base is oriented for heat flow in the axial direction; heat flow is perpendicular to the glue joints for axial samples. The radial counterpart was sectioned from the side of the subassembly and is oriented for heat flow parallel to the glue joints. The thermal conductivity of the fiberboard samples was measured using a Lasercomp Fox Series heat flow meter at a mean temperature of 25 °C with a 20 °C difference between the upper and lower plates.

A total of four samples (1 inch diameter x 1.8 inch height) were prepared from the side and base of the lower subassembly to evaluate the specific heat capacity of the fiberboard. The specific heat capacity was calculated in accordance with ASTM method C351 at a mean temperature of approximately 25 °C. Data were collected for a sample target temperature of 45 °C and a water temperature of approximately 5 °C. Each sample was tested three or four times and all results were averaged.

The mechanical properties of fiberboard samples (2 inch cube) were tested using an Instron 4507 compression tester at a crosshead speed of 1.9 inch/min. The load was applied either parallel or perpendicular to the fiberboard layers. Compression testing results provide data relevant to the evaluation of package resistance to crushing. The integrated area under the stress-strain curve up to 40% strain provides a relative measure of the energy absorption capability of each sample. The 40% strain level is arbitrary but provides a consistent point for comparison of fiberboard samples from different DE packages. The buckling strength provides additional comparison metric for samples tested in the parallel orientation.

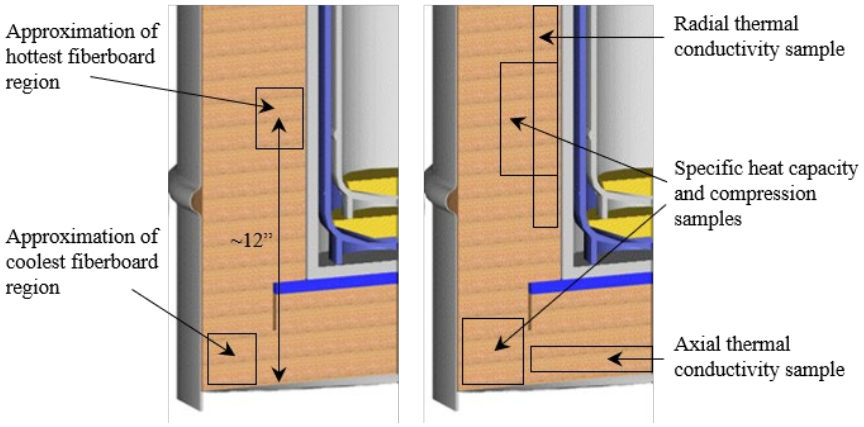

Figure 1. Depiction of fiberboard sections from the lower subassembly used for thermal and mechanical testing. Not to scale.

O-ring examination and testing: The dimensions of the O-rings were measured during DE. The minor diameter, or cross-section thickness, was measured for the radial (width between the O-ring inside and outside diameter) and axial (width between the top and bottom of the O-ring) thicknesses. The length was measured after cutting the O-ring and used as the circumference in the calculation for major diameter. The chemical composition was characterized using Fourier transform infrared spectroscopy (FTIR). The cross-section of the outer primary and secondary containment vessel (PCV and SCV) O-rings were

microscopically examined using a Keyence VR-3200 microscope and a Hitachi SU8200 Ultimate Cold Field Emission scanning electron microscope (SEM). The inner PCV O-ring was tensile tested using an MTS Criterion Model 43 with flat grips. The O-ring was elongated at a rate of 10 inch/min until 50% strain, where it was visually examined, and then elongated at 20 inch/min until it reached its breaking point. The compression set of the O-rings was calculated by assuming an initial minor diameter of 0.139 inch and an average groove depth in the lid of 0.0995 inch in the following equation,

$$\text{Compression set (\%)} = (0.139 - \text{radial thickness}) / (0.139\text{-}0.0995) * 100$$

Lead shield examination: The lead shield was visually examined for significant deformation, excessive corrosion and physical damage, and its dimensions were measured and compared to drawing requirements.

3.0 Results and Discussion

3.1 Upper and Lower Fiberboard Examination

The physical measurements of the fiberboard subassemblies are recorded in Table 1 and the dimension labels are depicted in Figure 6. The weight and dimensions of the fiberboard subassemblies taken during destructive examination are in good agreement with drawing requirements. The calculated densities of 0.271 and 0.283 g/cm^3 for the upper and lower subassemblies meet the limit for the criticality control function of >0.20 g/cm^3. The axial gap measured at SRNL of 1.021 inch slightly exceeds the 1 inch maximum criterion. The initial axial gap for 9975-02731 is unknown but the nominal axial gap is 0.8 inch. The increase is axial gap is likely due to changes in fiberboard moisture content and settling and compaction of fiberboard assemblies during service.

Table 1. Physical measurements and calculated density of package components

	Destructive examination						Nominal value [1, 13]
	Dimensions	0°	90°	180°	270°	Average	
	Axial gap (in)	1.028	1.071	1.003	0.980	1.021	< 1
Upper subassembly	UD1 (in)	17.804	17.829			17.817	17.7
	UD2 (in)	8.555	8.575			8.565	8.55
	UR1 (in)	3.051	3.054	3.029	3.032	3.042	3.075
	UR2 (in)	1.466	1.514	1.480	1.484	1.486	1.5
	UH1 (in)	7.281	7.208	7.256	7.247	7.248	7.1
	UH2 (in)	2.020	2.010	2.010	2.023	2.016	2.1
	UH3 (in)	4.964	4.940	4.980	4.974	4.965	5.0
	Weight	12.465 kg (27.481 lb)					
	Density	0.271 g/cm^3					> 0.21 g/cm^3
Lower subassembly	LD1 (in)	17.955	18.020			17.988	18.1
	LD2 (in)	8.470	8.472			8.471	8.45
	LR1 (in)	3.294	3.327	3.321	3.295	3.309	3.275
	LR2 (in)	1.506	1.511	1.506	1.504	1.507	1.55
	LH1 (in)	26.516	26.515	26.626	26.599	26.564	26.7
	LH2 (in)	20.535	20.323	20.310	20.322	20.373	20.4
	LH3 (in)	1.982	1.989	2.000	2.008	1.995	2.0
	Weight	26.244 kg (57.858 lb)					
	Density	0.283 g/cm^3					> 0.21 g/cm^3
Lead shield	OD (in)	8.352	8.358			8.356	8.252 – 8.35
	ID1 (in)	7.254	7.250			7.252	7.25 – 7.26
	ID2 (in)	7.243	7.263			7.254	7.24 – 7.26
	R (in)	0.593	0.597	0.592	0.595	0.594	> 0.506
	H (in)	24.724	24.717	24.718	24.714	24.719	24.59 – 24.7

Dark discoloration was noted on the upper fiberboard subassembly during unpackaging in KAC (Figure 2). The large stain on the flat surface and side of the upper fiberboard indicates a substance was spilled on the fiberboard assembly and then dried. Similar but smaller dark stains have been observed along glue joints in other DE packages and the stains were attributed to dried and smeared glue [11-12]. Figure 3 shows pictures of the upper fiberboard assembly with excess dried glue residue. Chemical analysis of the discolored fiberboard was performed using FTIR. Samples were taken of the upper fiberboard assembly from areas with and without the discoloration. Elmer's® Carpenter's wood glue, a water-based poly(vinyl acetate) adhesive used in laminating the fiberboard, was applied on a separate fiberboard sample. The FTIR spectra of the fiberboard samples and the wood glue are presented in Figure 4. The FTIR spectra of the fiberboard samples with and without discoloration are very similar although the peaks are more pronounced for the former. This could be due to the contribution from poly(vinyl acetate) adhesive as the glue has peaks that overlap with the fiberboard sample, such as at 2924 cm^{-1} (-CH), 1422 cm^{-1} ($-CH_2$), and 1024 cm^{-1} (-C-O). Optical microscope images show both the discolored fiberboard and sample with dried wood glue have glossy surfaces (Figure A-1). The visual and chemical examination of the upper fiberboard assembly indicate the discoloration is consistent with dried wood glue residue.

Figure 2. Pictures of upper fiberboard subassembly with large discoloration attributed to dried glue (photos taken by KAC personnel during unpackaging).

Figure 3. Pictures of (a) upper fiberboard assembly with discoloration and (b) close-up of excess dried glue in the fiberboard junction.

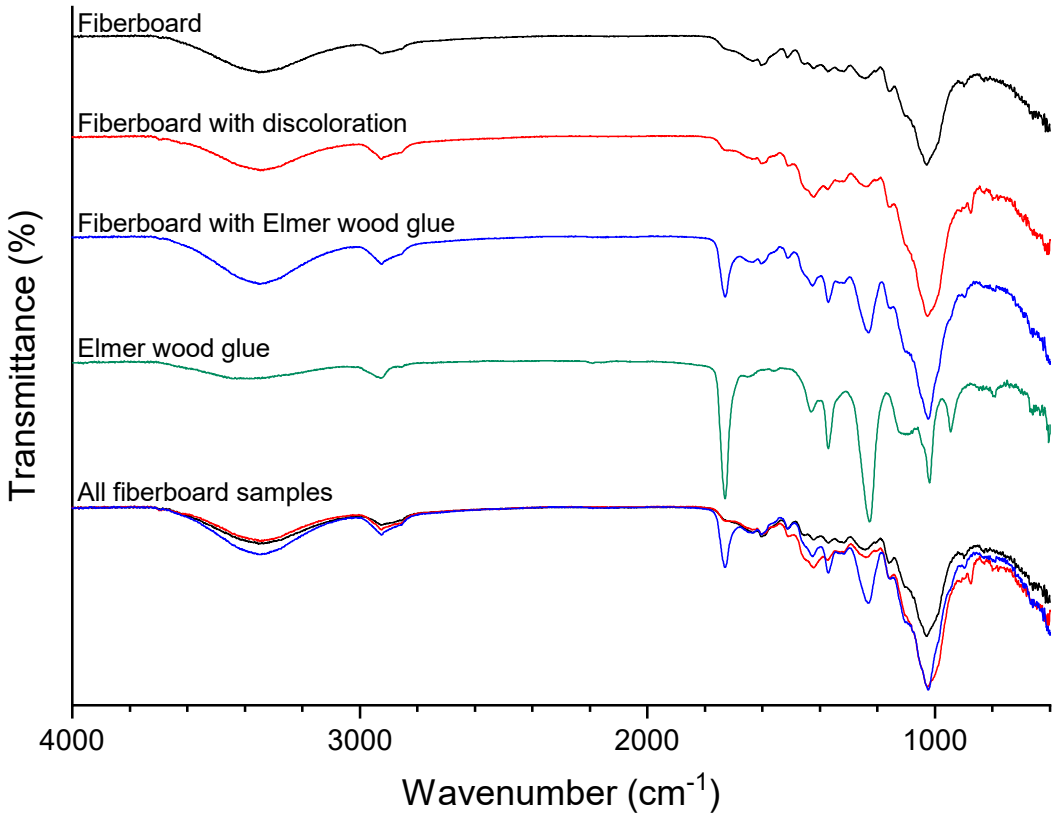

Figure 4. FTIR spectra of the upper fiberboard samples with and without discoloration, and with applied Elmer wood glue.

The lower fiberboard assembly came out smoothly from the drum and appeared visually consistent with undamaged fiberboard (Figure 5). There was no dark staining from dried glue residue on the surfaces. A white band was observed in the cavity of the fiberboard assembly due to contact with the corrosion products on the lead shield. The contact with the lead shield was superficial as the lead shield was lifted easily from the fiberboard assembly.

The moisture content of fiberboard assemblies will affect its physical, thermal, and mechanical properties. Moisture measurements of fiberboard assemblies could corroborate laboratory test results and trends with behavior in packages stored in KAC. Fiberboard moisture content was measured during SRNL examinations and presented in Figure 6a. The fiberboard between the upper and lower bearing plates has an average moisture content of approximately 12% WME, which is typical of the average moisture content seen in many packages. The humidity of the surrounding air and fiberboard moisture content along the fiberboard OD surface are presented in Figure 6b. The 9975-02731 fiberboard moisture data show reasonable agreement with the trend from fiberboard laboratory samples and other previously examined DE packages. In general, DE package data are minorly offset to higher moisture content from laboratory data, likely due to the differences in sample size and ability to retain moisture; DE package data are from full subassemblies while lab samples are 2 inch cubes.

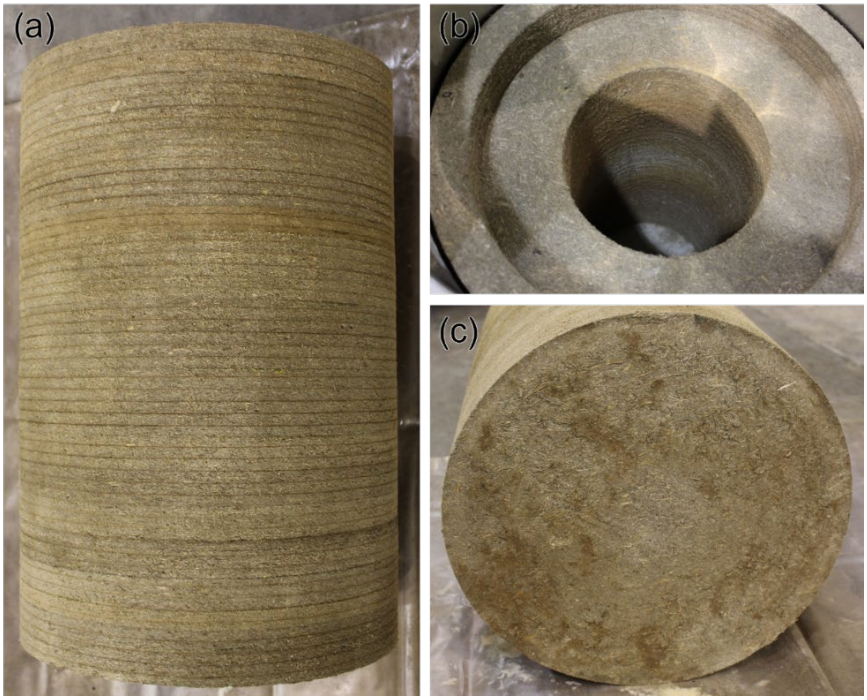

Figure 5. Pictures of (a) side, (b) inside, and (c) bottom of the lower fiberboard assembly.

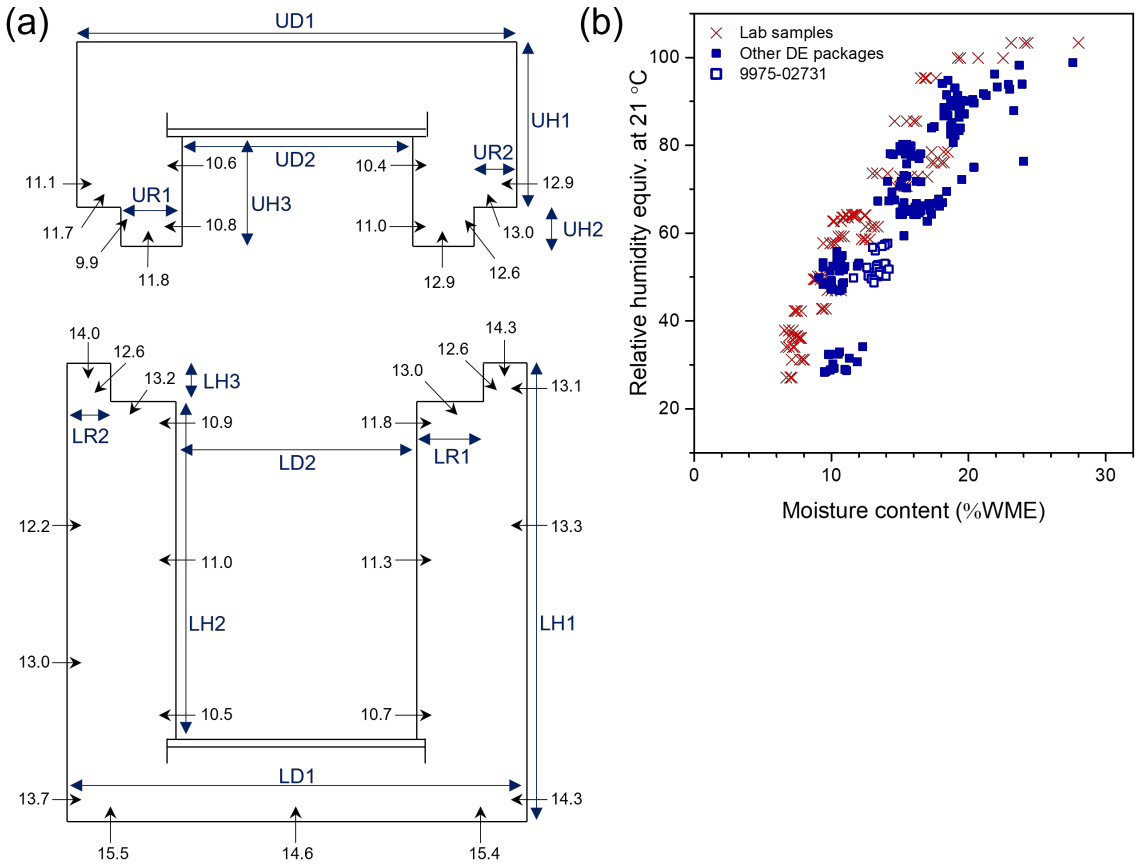

Figure 6. (a) Moisture content (% WME) data of the fiberboard subassemblies. (b) Plot of measured fiberboard moisture content and the relative humidity of the adjacent air.

Physical measurements and testing results for 9975-02731 fiberboard test samples are recorded in Table 2. The thermal conductivities, λ, are 0.0358 and 0.0605 Btu/hr·ft·°F for the axial and radial samples, respectively. These values are within the acceptance range and in reasonable agreement with DE package and laboratory baseline data as shown in Figure 7a. The average specific heat capacities were 1383 and 1855 J/kg·K for the base and side samples, respectively (Figure 7b). Multiplying the specific heat capacity, C_p, by the density of the lower subassembly (283 kg/m^3) and converting units yields an average heat capacity of 5.835 Btu/ft^3·°F for the two base samples and 7.826 Btu/ft^3·°F for the two side samples. These fiberboard samples meet the required minimum specific heat capacity of 3 Btu/ft^3·°F and are consistent with previous DE packages and laboratory baseline data. Thermal conductivity and specific heat capacity increase with increasing moisture content of fiberboard samples. The fiberboard subassembly, used for over 13.8 years as a thermal insulator in 9975-02731, met the thermal property acceptance criteria.

Compression test results are shown in Figure A-2 and Figure 8 along with baseline fiberboard data. A series of photographs showing typical compression behavior of the sample under parallel orientation is presented in Figure A-3. As shown in Figure 8, energy absorption and buckling strength tend to decrease with increasing moisture content. The samples from 9975-02731 are consistent with other fiberboard samples, although on the lower end of the trend compared to other DE packages (Figure 8).

Fiberboard properties can change over time due to moisture and thermo-oxidative degradation. Laboratory fiberboard testing identified a threshold of 125 °F for degradation and no significant degradation is expected below 120 °F [14]. The average sidewall fiberboard temperature in 9975-02731 was estimated using the method described in Ref. 15 by adding the conservative average ambient temperature in KAC in a storage array (95 °F [16]) and the heat contribution from the package contents (fiberboard sidewall temperature is 49 °F warmer than ambient at 19 watts). For 9975-02731, the average sidewall fiberboard temperature would have been 95 °F + 49 °F*(3.0 W/19 W) = 103 °F, which is below the fiberboard degradation threshold. As discussed above, the fiberboard samples from 9975-02731, stored in KAC for 13.8 years, satisfy acceptance criteria for physical and thermal properties.

Table 2. Physical measurements and testing data for fiberboard test samples

	Sample	Moisture content (%WME)	Weight (g)	Density (g/cm^3)	Testing results		
					Experimental		Allowed values [9]
Compression	Base 1 (‖)	11.0	37.9193	0.275	Absorbed energy (ksi)	0.0537	
	Base 2 (‖)	11.4	39.7318	0.284		0.0572	
	Base 3 (⊥)	10.8	38.9094	0.281		0.0496	
	Base 4 (⊥)	10.8	39.1634	0.287		0.0482	
	Side 1 (‖)	10.8	36.7062	0.274		0.0353	
	Side 2 (‖)	10.1	38.2708	0.288		0.0347	
	Side 3 (⊥)	10.8	37.4846	0.284		0.0289	
	Side 4 (⊥)	10.8	36.0820	0.276		0.0277	
Thermal conductivity	Base (axial)	10.7	367.6	0.283	λ (Btu/hr·ft·°F)	0.0358	0.032 – 0.040
	Side (radial)	10.8	341.2	0.273		0.0605	0.053 – 0.067
Heat capacity	SHC base 1	9.8			C_p (Btu/ft^3·°F)	5.848	> 3
	SHC base 2	9.8				5.821	
	SHC side 1	9.4				7.791	
	SHC side 2	9.8				7.860	

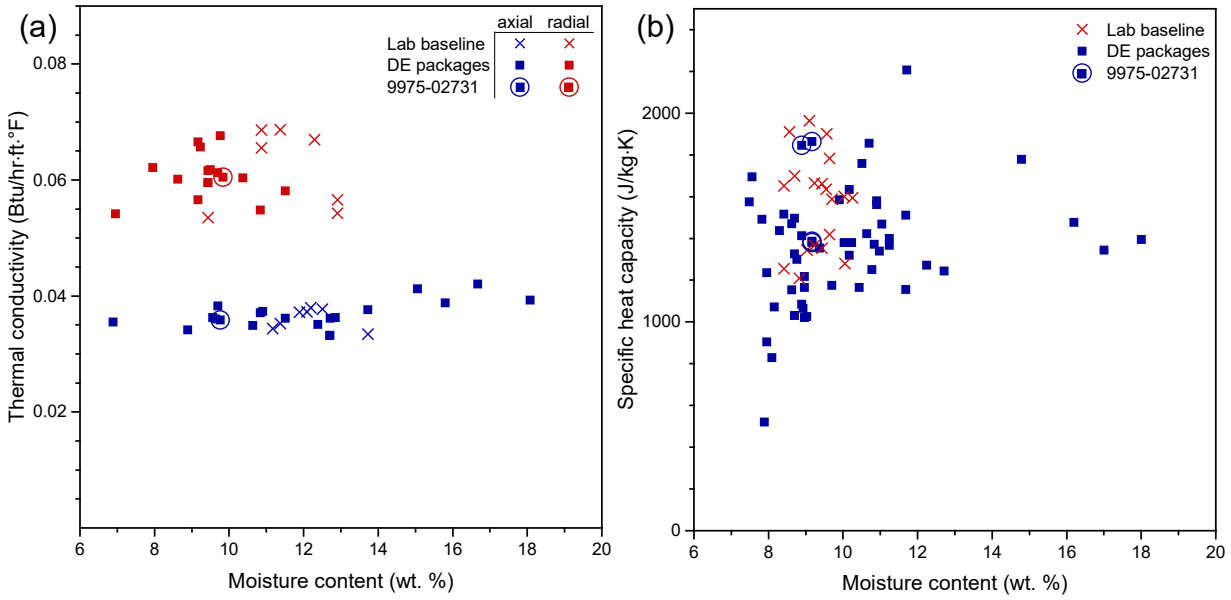

Figure 7. Thermal properties of fiberboard from destructively examined packages and laboratory baseline samples including (a) thermal conductivity and (b) specific heat capacity.

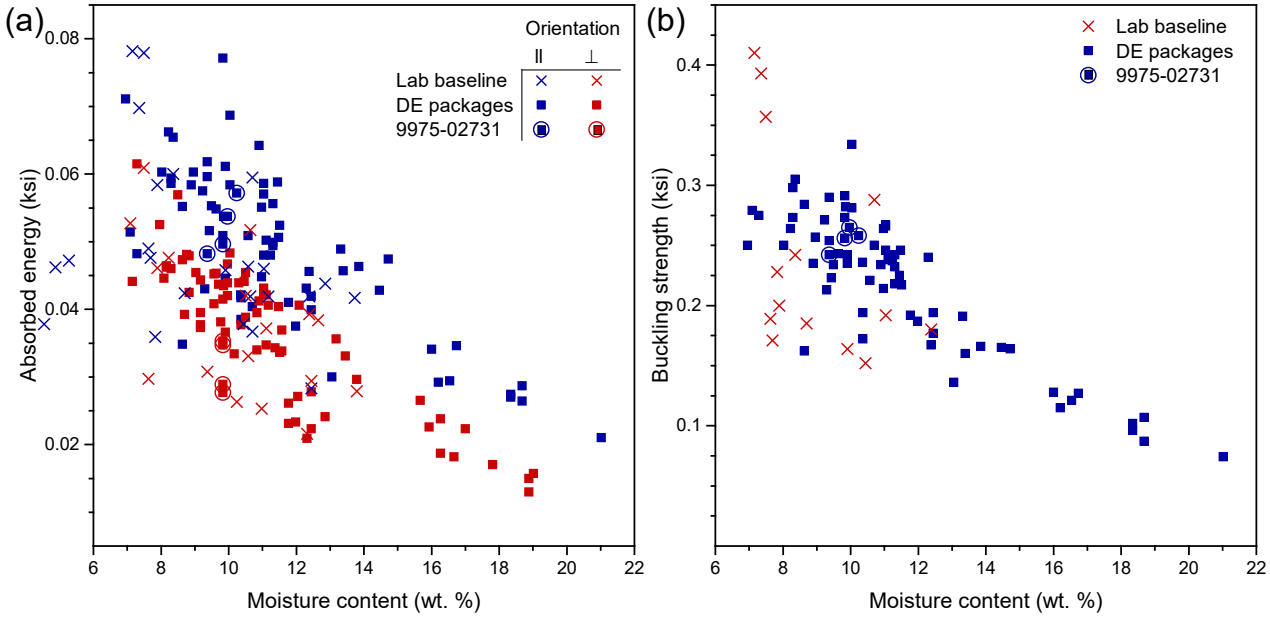

Figure 8. Calculated (a) absorbed energy and (b) buckling strength from compression testing of destructively examined packages and laboratory fiberboard samples.

3.2 Lead Shield Examination

The entire surface of the lead shield was visually examined, and it was found to be free from significant deformation, excessive corrosion (*e.g.,* blistering, flaking) and physical damage. The surface was covered with a layer of white, gray, and tan corrosion products as observed on other packages (Figure 9). The lead shield has one noticeable brown band that appear to correspond to the observed white band on the inside cavity of the lower fiberboard assembly (Figure 5b). There were sporadic clusters of small, raised corrosion

products on the surface. The physical measurements of the lead shield are recorded in Table 1 and the dimension labels are depicted in Figure 9e. All but two dimensions are consistent with drawing requirements; the OD is 0.006 inch greater than the drawing specifications of 8.252-8.35 inch, and the height of the shield is 0.019 inch greater than the drawing specification of 24.7 inch.

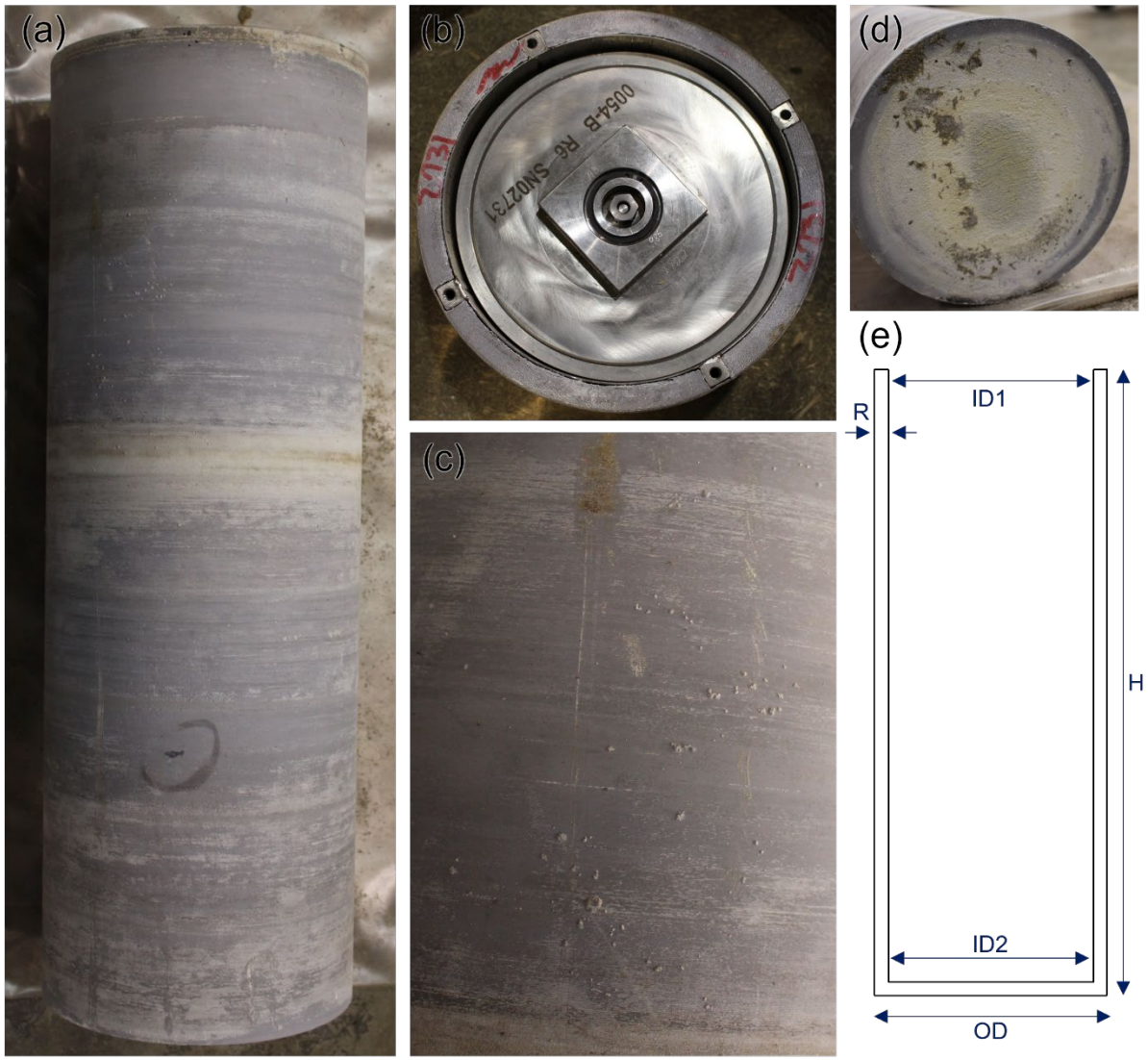

Figure 9. Pictures of (a) lead shield, (b) top of shield, (c) close-up of raised corrosion products, and (d) bottom of shield. (e) Drawing of lead shield and dimension labels.

3.3 O-ring Examination

The physical measurements of the four O-rings from 9975-02731 are recorded in Table 3. The average minor diameter for each O-ring is within the specified tolerances for new O-rings. The major inside diameters (ID) for the PCV and SCV outer O-rings are greater than specifications for new O-rings due to the permanent stretch from the lid diameter. Compression set for the four O-rings ranged from 4-15% when measured at SRNL 98 days after the package was opened in KAC. Compression set decreases with time as the elastomer continues to relax and typically reaches an equilibrium value after ~30 days. An O-ring that completely recovers to its original thickness has a compression set of 0%. The compression set values are within the range of values measured for O-rings from other DE packages (Figure A-4).

Table 3. Physical measurements of O-rings

Dimensions		PCV outer O-ring		SCV outer O-ring		PCV inner O-ring		SCV inner O-ring	
		Radial	Axial	Radial	Axial	Radial	Axial	Radial	Axial
Thickness (in)	0°	0.1370	0.1360	0.1315	0.1350	0.1390	0.1365	0.1310	0.1360
	45°	0.1390	0.1360	0.1315	0.1350	0.1415	0.1360	0.1315	0.1360
	90°	0.1385	0.1355	0.1350	0.1345	0.1360	0.1360	0.1325	0.1355
	135°	0.1370	0.1360	0.1345	0.1345	0.1335	0.1370	0.1355	0.1340
	180°	0.1370	0.1365	0.1295	0.1345	0.1330	0.1360	0.1355	0.1335
	225°	0.1370	0.1370	0.1335	0.1345	0.1300	0.1355	0.1350	0.1335
	270°	0.1370	0.1360	0.1350	0.1345	0.1300	0.1330	0.1315	0.1345
	315°	0.1370	0.1350	0.1340	0.1355	0.1335	0.1350	0.1305	0.1360
	Average	*0.1374*	*0.1360*	*0.1331*	*0.1348*	*0.1346*	*0.1356*	*0.1329*	*0.1349*
		0.1367		*0.1339*		*0.1351*		*0.1339*	
	Nominal value	0.139 ± 0.005		0.139 ± 0.005					
Length		14 $^{5}/_{16}$ in		17 $^{17}/_{32}$ in					
Calc. major dia.		4.556 in		5.580 in					
New major dia.		4.234 ± 0.045 in		5.234 ± 0.054 in					
Weight		6.0108 g		7.1837 g					
Calc. volume		0.2101 in^3		0.2469 in^3					
Calc. density		1.746 g/cm^3		1.776 g/cm^3					
Hardness	1, M-Scale	74.2		73.4		72.0		75.6	
	2, M-Scale	71.4		75.6		66.2		76.4	
	3, M-Scale	71.2		71.2		69.4		73.6	
	4, M-Scale	74.2		73.0		76.6		72.4	
	5, M-Scale	71.2		78.0		74.4		73.6	
	Average	*72.4*		*74.2*		*71.7*		*74.3*	
Compression set (%)		4.1		14.9		11.1		15.4	

FTIR spectra of the O-rings were indistinguishable from each other and consistent with a Viton® type fluoroelastomer (Figure A-5). Optical and SEM images of the O-ring cross sections identified a distribution of very small particles throughout the outer PCV and SCV O-rings (Figure A-6 and Figure A-7). EDS identified small amounts of aluminum, silicon, and zinc, which are likely from additives in the formulation (*e.g.,* ZnO). Tensile test results are shown in Figure 10, and no cracks or other signs of degradation were observed during elongation to 50% strain. The PCV inner O-ring failed after reaching 225% elongation with a tensile strength of ~1.9 ksi. These values are consistent with the O-rings from other DE packages and comparable with the baseline Viton® GLT mechanical properties.

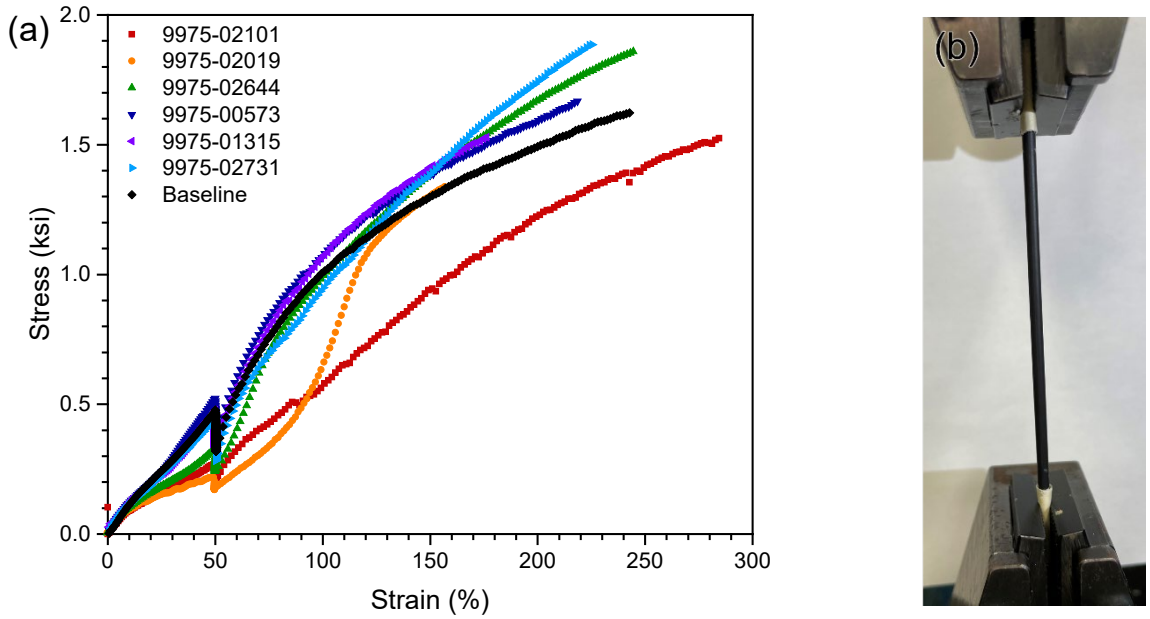

Figure 10. Tensile (a) stress-strain curves for PCV inner O-rings from DE packages and picture (b) of tensile testing at 50% stretch using flat yarn grips for 9975-02731.

3.4 General Observations

All metallic components were visually examined. Various fabrication markings were stamped or engraved on the containment vessels and lids, consistent with previous DE observations. The interior of the stainless steel drum had regions of light staining or possible minor corrosion. No other signs of physical damage were observed on the metallic components.

4.0 Conclusions

Destructive and non-destructive examinations were completed on package 9975-02731, used in the storage of nuclear materials in KAC for 13.8 years. During unpackaging in KAC, a large discoloration was observed on the upper fiberboard subassembly. Visual examination of the fiberboard assembly and analysis of the discolored fiberboard indicate the discoloration was due to dried wood glue. There was a layer of corrosion products on the surface of the lead shield but no evidence of excessive blistering, flaking, or spalling. Lead corrosion can be catalyzed by products of fiberboard degradation, however, there were no indications during the examination of degraded fiberboard. The results of testing the physical, thermal, and mechanical properties of the lower fiberboard subassembly showed it met the acceptance criteria and/or were consistent with results and trends from previous DE packages. The examination of the O-rings did not reveal any signs of degradation or physical damage. Besides minor and expected corrosion, there was no evidence of a degraded condition in package 9975-02731.

All findings will be reviewed by Nuclear Materials Management for potential impact on the continued storage of other packages in KAC.

5.0 References

1. Safety Analysis Report for Packaging Model 9975, Savannah River Nuclear Solutions, S-SARP-G-00003, Rev. 4, 2015.
2. K-Area Complex Documented Safety Analysis, Savannah River Nuclear Solutions, WSRC-SA-2002-00005, Rev. 16, 2021.
3. Hensel, S. J., Evaluation of 9975 Shipping Package Analyses for 20 Year Storage of 3013 Containers in KAC, Savannah River Nuclear Solutions, M-ESR-K-00073, 2017.
4. Grimm, R. J., 9975 Shipping Package/ 3013 Container 20 Year Life Extension Summary, Savannah River Nuclear Solutions, G-ESR-K-00204, 2017.
5. O'Grady, A. J., 9975 Shipping Package/3013 40 Year Life Extension Summary, Savannah River Nuclear Solutions, G-ESR-K-00253, 2022.
6. Escobar, A. J.; Hensel, S. J., 9975 Shipping Package/non-3013 Container 20 Year Life Extension Summary, Savannah River Nuclear Solutions, G-ESR-K-00231, 2019.
7. Kiflu, B. B., Summary and Matrix: 9975 Shipping Package Qualification Program for Extended Storage of Plutonium in the K-Area Complex, Savannah River Nuclear Solutions, SRNS-TR-2008-00290, Rev. 2, 2016.
8. Escobar, A. J., Savannah River Site Surveillance Program for the Storage of 9975/3013 Plutonium Packages in KAC, Savannah River Nuclear Solutions, WSRC-TR-2001-00286, Rev. 10, 2021.
9. Daugherty, W. L., Task Technical and Quality Assurance Plan for Destructive Examination of a 9975 Package from Field Surveillance Activities, Savannah River National Laboratory, WSRC-TR-2005-00135, Rev. 1, 2011.
10. Truong, T. T., Electronic Laboratory Notebook, Destructive examination of 9975-02731, Savannah River National Laboratory, L6004-00395-03.
11. Daugherty, W. L., Destructive examination of shipping package 9975-02101, Savannah River National Laboratory, SRNL-STI-2016-00209, 2016.
12. Truong, T. T., Destructive examination of shipping package 9975-00573, Savannah River National Laboratory, SRNL-STI-2019-00021, 2019.
13. 9975 Shipping Package Insulation Assembly, Subassemblies & Details, Savannah River National Laboratory, R-R2-F-0019, Rev. 8, 2008.
14. Daugherty, W. L.; Truong, T. T., Status report - Fiberboard properties and degradation rates for storage of the 9975 shipping package in KAC, Savannah River National Laboratory, SRNL-STI-2018-00127, 2018.
15. Daugherty, W. L., Destructive examination of shipping package 9975-02644, Savannah River National Laboratory, SRNL-STI-2017-00666, 2017.
16. Kiflu, B. B., The Initial and 20-year Service Thermal Performances of the 9975 Shipping Packages due to Fire-Drop-Smoldering Accidents in KAC, M-CLC-K-00788, 2017.
17. Daugherty, W. L.; Truong, T. T., Examination of Shipping Package 9975-04194, Savannah River National Laboratory, SRNL-STI-2018-00228, 2018.
18. Truong, T. T., Examination of Shipping Package 9975-01378, Savannah River National Laboratory, SRNL-STI-2019-00230, 2019.
19. 9975 Shipping Package Shielding, Savannah River National Laboratory, R-R2-F-0020, Rev. 11, 2009.

Appendix A. Supplemental Information

Measurement Uncertainties:
Numerous measurements were made during the destructive examination of package 9975-02731 for trending purposes or comparison to inspection criteria. All measurements which are compared to inspection criteria were made with calibrated instruments or were verified against calibrated instruments. The uncertainties associated with measurements and calculated results required to meet inspection criteria are discussed below. Uncertainties are provided at the 95% or 2σ confidence level unless otherwise stated.

Weight: The weight of each fiberboard subassembly was measured to a precision of 1 gram. The balance used was Measuring and Test Equipment (M&TE), and the calibration data show accuracy within 6 grams over the range of interest. A conservative net uncertainty of 7 grams was used.

Calipers: Three different calipers were used to measure component dimensions. Calibration data show accuracy within 0.004 inch for the calipers. In addition, operator bias can affect measurement accuracy through applied contact load, especially on fiberboard samples that have some give. It is estimated that the total uncertainty for fiberboard measurements is no greater than ± 0.004 inch for the 8 inch calipers, ± 0.008 inch for the 24 inch calipers, ± 0.01 inch for the 40 inch calipers. Dimension ID2 on the lead shield was captured with manual swing calipers, and it is estimated that the uncertainty is ± 0.004 inch.

Thermal conductivity: The specifications of the Fox 300 and Fox 314 thermal conductivity instruments include a stated accuracy of ~1% and 2%, respectively. Measurement of thermal conductivity of a calibration standard was accurate to within 1% on either instrument. An uncertainty of 3% will be conservatively assumed for the current measurements on either instrument.

Heat capacity: Consistency of operator technique is the biggest contribution to measurement error. Four measurements were taken on each of the two samples from the two regions. The variation for each sample ranged from 18 to 24%. The combined uncertainty on the average of two samples is 15% for the base region and 14% for the side region.

A standard error propagation formula for random errors is used to calculate the final result uncertainty. Calculation results and their uncertainties are summarized below:

Upper fiberboard subassembly volume = 29660 ± 40 cm^3
Upper fiberboard subassembly density = 0.271 ± 0.001 g/cm^3
Lower fiberboard subassembly volume = 84980 ± 113 cm^3
Lower fiberboard subassembly density = 0.283 ± 0.001 g/cm^3
Shield radial thickness at bottom = 0.594 ± 0.003 in
Thermal conductivity (radial) = 0.0605 ± 0.002 Btu/hr·ft·°F
Thermal conductivity (axial) = 0.0358 ± 0.001 Btu/hr·ft·°F
Heat capacity (base) = 5.8 ± 0.9 $Btu/ft^3 \cdot °F$
Heat capacity (side) = 7.8 ± 1.1 $Btu/ft^3 \cdot °F$

Figure A-1. Optical microscope images of (a) upper fiberboard, (b) discolored fiberboard, and (c) fiberboard with dried Elmer's® wood glue.

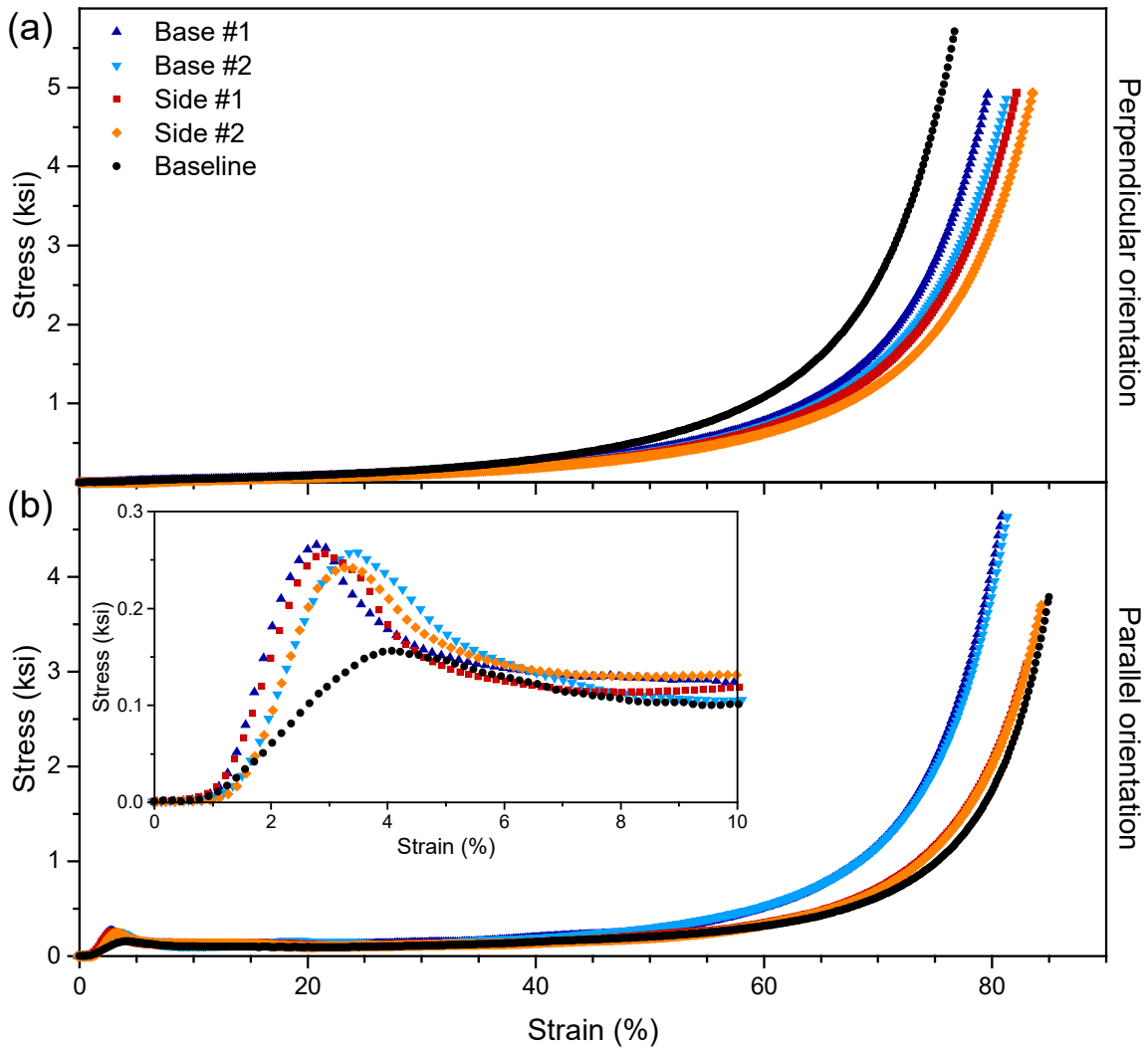

Figure A-2. Stress-strain curves for the compression of 9975-02731 fiberboard samples in the (a) perpendicular and (b) parallel orientations, and baseline data from an unaged fiberboard assembly. The inset graph shows the linear elastic and buckling region for fiberboard samples compressed in parallel orientation.

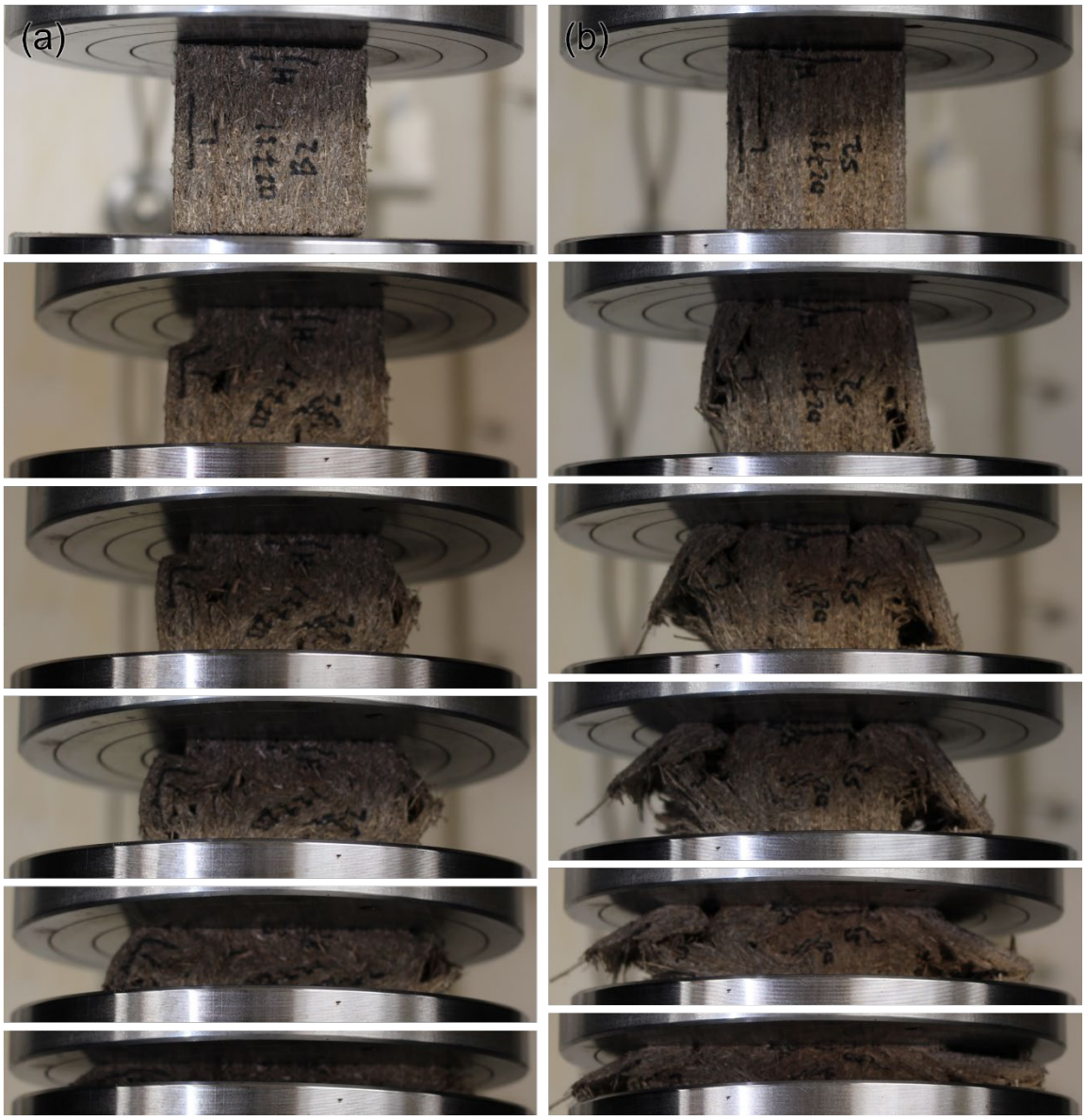

Figure A-3. Pictures of compression testing, in the parallel orientation, of fiberboard samples from the (a) base and (b) side of the lower subassembly.

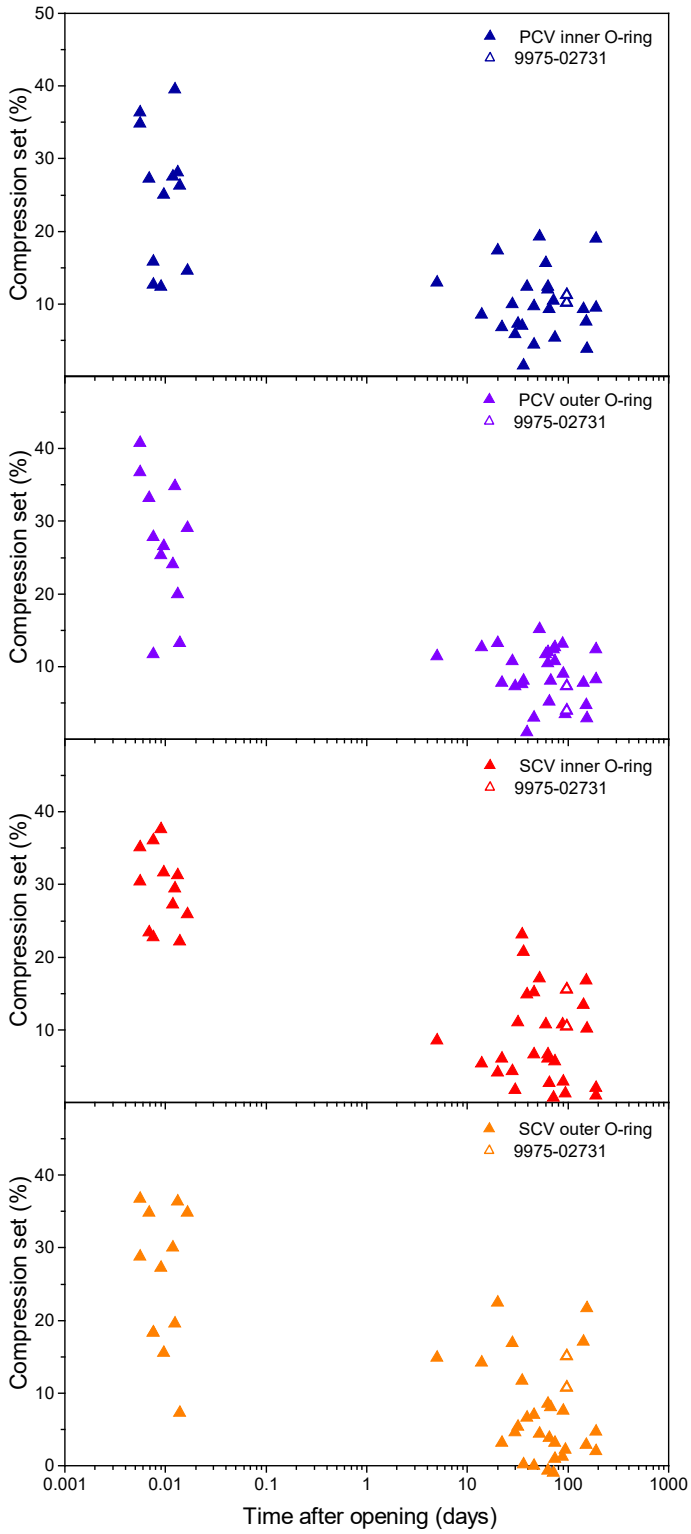

Figure A-4. Compression set of SCV and PCV O-rings from 9975-02731 and other DE packages.

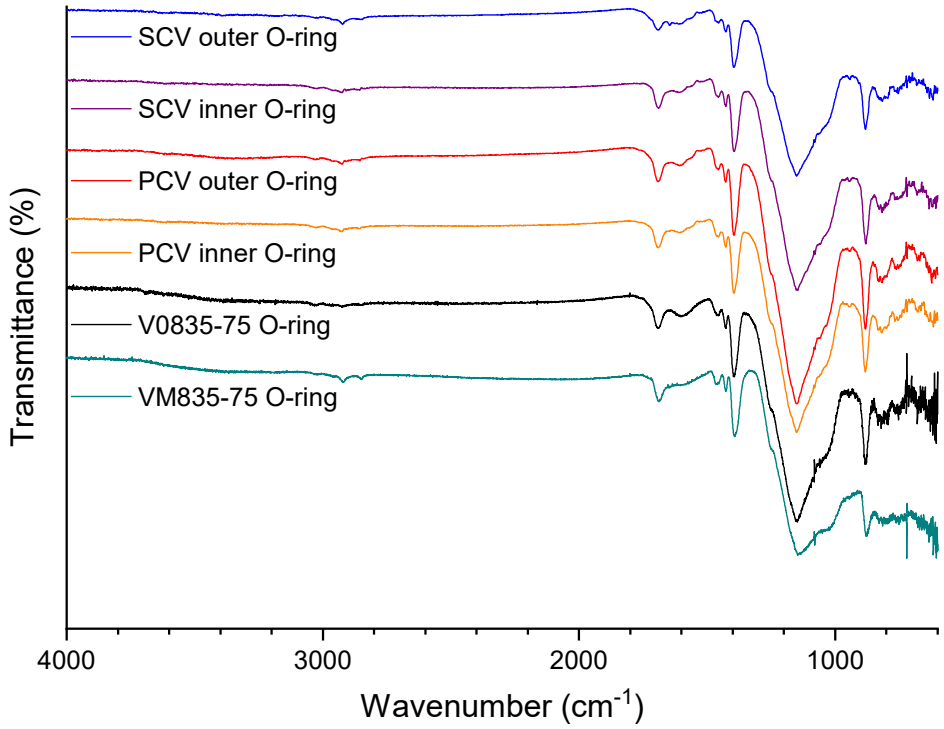

Figure A-5. FTIR spectra of the 9975-02731 SCV and PCV O-rings.

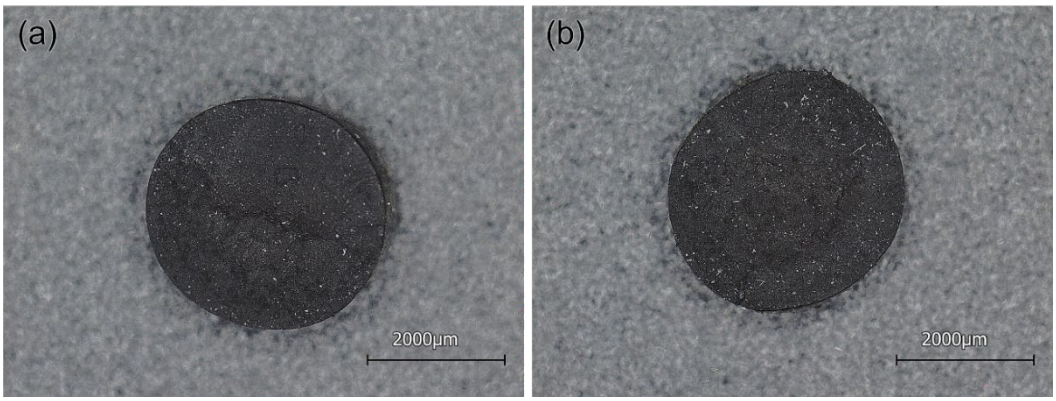

Figure A-6. Optical cross section of the (a) PCV outer and (b) SCV outer O-rings.

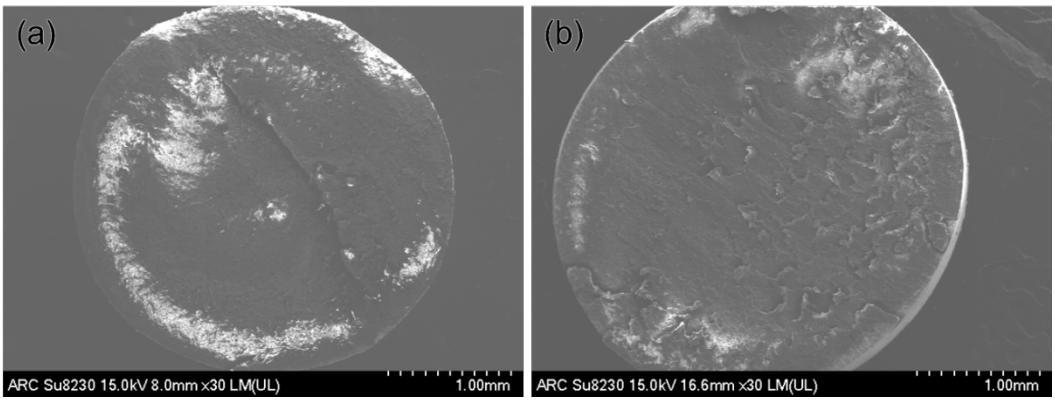

Figure A-7. SEM cross section images of (a) PCV outer and (b) SCV outer O-rings.

Distribution:

R. J. Bayer, 705-K
E. M. Chrisler, 705-K
R. E. Fuentes, 773-A
R. J. Grimm, 705-K
S. J. Hensel, 705-K
S. L. Hudlow, 705-K
J. M. Jordan, 705-K
M. D. Kranjc, 730-A
D. R. Leduc, 730-A
J. M. Licea-Yanez, 730-A
Z. Lowe, 773-51A
J. W. McEvoy, 707-C
K. Moeller, 705-K
A. J. O'Grady, 705-K
R. A. Osborne, 705-K
F. M. Pennebaker, 773-A
M. M. Reigel, 773-A
T. E. Skidmore, 730-A
B. J. Wiedenman, 773-42A
Document Control